Why is *Trichodesmium* abundant in the Kuroshio?

T. Shiozaki[1,2], S. Takeda[1,3], S. Itoh[2], T. Kodama[1,4], X. Liu[1,5], F. Hashihama[6], K. Furuya[1]

[1]{Department of Aquatic Bioscience, Graduate School of Agricultural and Life Sciences, The University of Tokyo, Tokyo, 113-8657, Japan}

[2]{Atmosphere and Ocean Research Institute, The University of Tokyo, Chiba, 277-8564, Japan}

[3]{Faculty of Fisheries, Nagasaki University, Nagasaki, 852-8521, Japan}

[4]{Japan Sea National Fisheries Research Institute, Fisheries Research Agency, Niigata, 951-8121, Japan}

[5]{College of Ocean and Earth Sciences, Xiamen University, Xiamen, 361005, China}

[6]{Department of Ocean Sciences, Tokyo University of Marine Science and Technology, Tokyo, 108-8477, Japan}

Corresponding to: T. Shiozaki (shiozaki@aori.u-tokyo.ac.jp)

Abstract

The genus *Trichodesmium* is recognized as an abundant and major diazotroph in the Kuroshio, but the reason for this remains unclear. The present study investigated the abundance of *Trichodesmium* spp. and nitrogen fixation together with concentrations of dissolved iron and phosphate in the Kuroshio and its marginal seas. We performed the observations near the Miyako Islands, which form part of the Ryukyu Islands, situated along the Kuroshio, since our satellite analysis suggested that material transport could occur from the islands to the Kuroshio. *Trichodesmium* spp. bloomed (>20,000 filaments L^{-1}) near the Miyako Islands, abundance was high in the Kuroshio and the Kuroshio bifurcation region of the East China Sea, but was low in the Philippine Sea. The abundance of *Trichodesmium* spp. was significantly correlated with the total nitrogen fixation activity. The surface concentrations of dissolved iron (0.19–0.89 nM) and phosphate (<3–36 nM) were similar for all of the study areas, indicating that the nutrient distribution could not explain the spatial differences in *Trichodesmium* spp. abundance and nitrogen fixation. Numerical particle-tracking experiments simulated the transportation of water around the Ryukyu Islands to the Kuroshio. Our results indicate that *Trichodesmium* growing around the Ryukyu Islands could be advected into the Kuroshio.

1. Introduction

The Kuroshio is a western boundary current in the North Pacific Ocean that originates in the North Equatorial Current and bifurcates to the east of the Philippines. The main stream of the Kuroshio enters the East China Sea (ECS) northeast of Taiwan, flows out through the Tokara Strait, and runs along the Japanese islands of Shikoku and Honshu. While the Kuroshio and its adjacent waters are characterized by highly oligotrophic conditions, phytoplankton and zooplankton communities in the Kuroshio are distinct compared to those from adjacent waters (McGowan, 1971). McGowan (1971) suggested that some plankton species are delivered by the Kuroshio to the north from the equatorial region.

The abundance of the cyanobacterial genus *Trichodesmium* in the Kuroshio is much higher than that in neighboring seas (Marumo and Asaoka, 1974). Because *Trichodesmium* is a major nitrogen fixer in the Kuroshio, it is believed to be the key genus for understanding the Kuroshio ecosystem (Chen et al., 2008, 2014; Shiozaki et al., 2014a). Nevertheless, the factors controlling the distribution of *Trichodesmium* in this region are poorly understood. Marine nitrogen fixation is thought to be regulated by the supply of iron and phosphorus (Mahaffey et al., 2005), and *Trichodesmium* thrives in iron-rich oligotrophic regions (Moore et al., 2009; Shiozaki et al., 2010,

2014b). A major source of iron in the ocean is atmospheric dust deposition (Jickells et al., 2005; Mahowald et al., 2009). Modeling studies indicate that dust deposition in the western North Pacific decreases exponentially from the continental shelf to the Philippine Sea (Jickells et al., 2005; Mahowald et al., 2009), and hence, deposition is not as high in the Kuroshio as in the adjacent waters. As for phosphorus limitation, iron-enhanced nitrogen fixation causes phosphorus depletion, and the nitrogen fixation is consequently limited by phosphorus (Mather et al., 2008). The phosphate distribution has been examined in this study region using a conventional colorimetric method, and the surface phosphate concentration in the Kuroshio has been reported to be as low as that in the Philippine Sea (Chen, 2008). Therefore, the distinct high abundance of *Trichodesmium* in the Kuroshio is probably not explained by nutrient and trace metal concentrations; however, distributions of dissolved iron and phosphate at the nanomolar level have not been well studied in this region (Obata et al., 1997; Shiozaki et al., 2010; Kodama et al., 2011).

Nitrogen fixation by *Trichodesmium* has recently also been found to be active around oceanic islands; New Caledonia Island, Efate Island, Fiji Island, Tahiti Island, and Northern Mariana Islands (Shiozaki et al., 2010, 2013, 2014c; Lin et al., 2011). Furthermore, these studies demonstrated that abundant *Trichodesmium* is delivered by

72 the current to areas that are remote from the islands. Although this phenomenon was
73 noted in the western Pacific warm pool and western South Pacific, it can also occur in
74 and around the Kuroshio and may contribute to the distribution of *Trichodesmium* in
75 this region.

76 In the present study, we simultaneously determined *Trichodesmium* abundance
77 and bulk water nitrogen fixation together with concentrations of dissolved iron and
78 phosphate at the nanomolar level in the Kuroshio and its marginal seas. In addition,
79 we conducted intensive observations around the Miyako Islands section of the
80 Ryukyu Islands located close to the main stream of the Kuroshio.

81

82 ## 2. Materials and Methods

83 ### 2.1. Oceanographic database

84 Algal blooms in an oligotrophic region may indicate a nitrogen fixation hotspot
85 (Wilson and Qiu, 2008; Shiozaki et al., 2014c). To identify the locations of intensive
86 algal blooms, we used a dataset of chlorophyll (chl) *a* observed by satellite. According
87 to Wilson and Qiu (2008), an algal bloom in an oligotrophic region can be defined as
88 a chl *a* value >0.15 mg m^{-3} in summer. In the present study, we used 8-day,
89 moderate-resolution imaging spectroradiometer (MODIS) level 3 chl *a* with 9 km

90 resolution during summer between July 2003 and September 2009. We defined
91 summer as July through September. The bloom frequency for each pixel was
92 calculated from the ratio of counts in which chl *a* was >0.15 mg m^{-3} to the total
93 counts in which chl *a* was detected.

94 To examine the current field, geoelectrokinetograph and ship-mounted acoustic
95 Doppler current profiler (ADCP) data from the uppermost layer for the summers
96 between 1953 and 2008 were obtained from the Japan Oceanographic Data Center
97 (http://www.jodc.go.jp). Regridding, removal of anomalous values, and smoothing of
98 the dataset were performed as described by Isobe (2008).

99

100 ## 2.2. **Cruise observations**

101 Experiments were conducted during summer on-board the R/V *Tansei-maru*
102 (KT-06-21, September 9–17, 2006; KT-07-22, September 5–13, 2007; KT-09-17,
103 September 8–13, 2009; KT-10-19, September 4–12, 2010) and the T/V
104 *Nagasaki-maru* (242, July 19–28, 2007) (Fig. 1a, Table S1). The stations during the
105 KT-06-21, KT-07-22, and *Nagasaki-maru* 242 cruises were divided into three areas
106 based on the temperature-salinity diagram (see Fig.2 of Shiozaki et al., 2011): the
107 ECS, Kuroshio, and Philippine Sea. During the KT-09-17 cruise, we conducted

experiments around the Miyako Islands which were distinguished from the other three areas. During the KT-10-19 cruise, we performed observations in the ECS, the Kuroshio, and around the Miyako Islands (Liu et al., 2013).

2.2.1. **Light intensity, hydrography, nutrients, and chl *a***

Water samples for all of the experiments, with the exception of determination of the dissolved iron concentration, were collected using an acid-cleaned bucket and Niskin-X bottles. The depth profile of light intensity was determined immediately before the water sampling using a light sensor (during the KT-06-22, KT-07-21, KT-09-17, and KT-10-19 cruises) or an empirical equation (during the *Nagasaki-maru* 242 cruise) (Shiozaki et al., 2011). Temperature and salinity profiles to a depth of 200 m were obtained using a conductivity, temperature, and depth (CTD) sensor. Mixed layer depth (MLD) was defined as the depth at which the sigma-t increased by 0.125 from its value at a depth of 10 m. Water samples for nitrate+nitrite (N+N) and phosphate were collected from 0, 10, 30, 40, 50, 60, 70, 80, 90, 100, 125, 150, and 200 m, and from depths at given light intensities. At all of the stations, the N+N and phosphate concentrations were determined at the nanomolar level using a supersensitive colorimetric system consisting of an AutoAnalyzer II (Technicon) and

126 Liquid Waveguide Capillary Cells (World Precision Instruments, USA) (Hashihama et
127 al., 2009). The detection limits of N+N and phosphate were both 3 nM. When the
128 concentration was greater than 0.1 μM, it was determined by conventional methods
129 using a TRAACS 2000 autoanalyzer (Bran:Luebbe, UK). In addition to the
130 observations at the stations, temperature, salinity, and the *in vivo* chl fluorescence of
131 the surface water were monitored continuously during the cruises by a
132 thermosalinograph (Ocean Seven, Idronaut, Italy) and a fluorometer (Minitracka,
133 Chelsea, UK).
134
135 ### 2.2.2. **Dissolved iron**
136 Water was sampled to estimate the dissolved iron concentration from 0.5-m depth
137 during the KT-06-21 and KT-07-22 cruises and from 10-m depth during the KT-09-17
138 cruise using an acid-cleaned Teflon bellows pump (AstiPure PFD2; Saint-Gobain)
139 with Teflon tubing (inner diameter = 12 mm). The water was filtered through an
140 acid-cleaned 0.22 μm pore filter (Millipak100; Millipore) connected to the in-line of
141 the Teflon tubing with a Teflon connector. Filtered seawater was collected in a 125
142 mL low-density polyethylene (LDPE) bottle (Nalgene, Nalge Nunc International),
143 which had been washed using following technique: the sample bottles were

144 sequentially cleaned by soaking in 5% alkali detergent for at least 2 days, in 4 N HCl
145 for at least 1 day, in 0.3 N metal analysis-grade HNO_3 at 60°C overnight, and finally,
146 in Milli-Q water at 60°C overnight. After rinsing with Milli-Q water, the bottles were
147 dried in a laminar flow space and stored in double plastic bags. The filtrate samples
148 were acidified to a pH <1.7 with trace-metal-grade HCl (Tamapure AA-100; Tama
149 Chemicals) in a Class-100 clean-air bench, and stored at room temperature for more
150 than 1 year.

151 The dissolved iron concentration was determined using an automatic Fe(III) flow
152 injection analytical system (Kimoto Electric Co., Ltd.) using a chelating resin
153 pre-concentration and chemiluminescence detection method (Obata et al., 1993). A
154 buffer solution of 10 M formic acid and 2.4 M ammonium formate was added to the
155 samples. The sample pH was adjusted to 3.0 with 20% ammonium hydroxide
156 (NH_4OH; Tamapure AA-10; Tama Chemicals) immediately prior to analysis. The
157 detection limit of this method was 0.05 nM. The SAFe reference standards S1 and D2
158 were measured during the course of sample analysis, and the results were within the
159 range of the published consensus values: S1 = 0.097 ± 0.043 nM and D2 = 0.91 ±
160 0.17 nM (Johnson et al., 2007).

161

2.2.3. **Nitrogen fixation and abundance of *Trichodesmium* spp.**

Samples for the incubation experiments were collected vertically at all of the stations, except at Sts. T0621, GN-3, and T0905, where samples were only collected from the surface. All samples were collected in duplicate in acid-cleaned 4.5-L polycarbonate bottles. During the *Nagasaki-maru* 242 cruise, water samples were collected from four different depths corresponding to 100%, 25%, 10%, and 1% of the surface light intensity. During the other cruises, samples were collected from a depth of 50% surface light intensity. Samples at 100% surface light intensity were collected from 0 m during all of the cruises, except during the KT-10-19 cruise in which the samples were collected from a depth of 5 m. The bulk water nitrogen fixation activity was determined based on primary production using a dual isotopic ($^{15}N_2$ and ^{13}C) technique (Shiozaki et al., 2009). After ^{13}C-labeled sodium bicarbonate (99 atom% ^{13}C; Cambridge Isotope Laboratories) was added to each bottle, 2 mL of $^{15}N_2$ gas (98 + atom% ^{15}N; SI Science Co. Japan) was injected directly into the incubation bottles through a septum using a gastight syringe. The bottles were covered with neutral-density screens to adjust the light level and incubated for 24 h in an on-deck incubator cooled by flowing surface seawater for 24 h. We determined the nitrogen fixation activity using the $^{15}N_2$ gas bubble addition method (Montoya et al., 1996).

This method is believed to underestimate the nitrogen fixation rate relative to the $^{15}N_2$ gas dissolution method (Mohr et al., 2010). The start time of incubation in this study varied at each station (Table S1). Considering daily periodicity of nitrogen fixation in each diazotroph (Zehr, 2011) and the time to reach equilibration of the $^{15}N_2$ gas bubble with seawater (>12 h, Mohr et al., 2010), the level of underestimation could vary at each station. Meanwhile, the level of underestimation is thought to be low in *Trichodesmium* dominant water because *Trichodesmium* can float to the top of the bottle and directly use the added $^{15}N_2$ in the bubble method (Großkopf et al., 2012). Although the bias of underestimation could not be estimated from the results in this study, the actual nitrogen fixation rate could be higher than the obtained rate.

A recent study demonstrated that commercial $^{15}N_2$ gas could be contaminated by ^{15}N-labeled nitrate and ammonium (Dabundo et al., 2014). We tested the contamination in $^{15}N_2$ gas produced by SI Science Co., Ltd., which was used (from different batch numbers) in the present study (see Supporting Information). Briefly, the $^{15}N_2$ gas was dissolved in aged subtropical surface water, and concentrations of nitrate, nitrite, and ammonium at the nanomolar levels were determined using supersensitive colorimetric systems. The results showed that there were no significant differences between the control and samples to which $^{15}N_2$ had been added (Fig. S1),

198 suggesting that the contamination of nitrate, nitrite, and ammonium in the $^{15}N_2$ gas
199 was insignificant (Supporting Information).

200 Water samples were collected for microscopic analysis at all light depths during
201 the *Nagasaki-maru* 242 and KT-07-21 cruises, and only from the surface during the
202 KT-06-22, KT-09-17, and KT-10-19 cruises. The samples were fixed using acidified
203 Lugol's solution. *Trichodesmium* spp. were counted using the Utermöhl method under
204 inverted microscope observation. *Trichodesmium* greater than ca. 300 μm in length
205 were counted as 1 filament and shorter lengths were counted as 0.5 filaments. In
206 addition, phytoplankton other than *Trichodesmium* spp. were identified from the
207 samples obtained during the KT-09-17 cruise.

208

209 ### 2.3. **Statistical analysis of environmental variables**

210 We used non-metric multi-dimensional scaling (nMDS) to investigate the spatial
211 differences in the environmental variables that could influence *Trichodesmium* growth
212 and bulk water nitrogen fixation; temperature, mixed layer depth, nitrate, dissolved
213 iron, and phosphate. The environmental variables were transformed by $\log_{10}(x + 1)$
214 prior to analysis. A dissimilarity/similarity matrix between stations was constructed
215 using the Bray-Curtis index. The nMDS was used to visualize similarities in the

environmental variables among the stations. An Analysis of Similarity (ANOSIM) was used to test the differences in the environmental variables among the stations.

2.4. **Numerical experiments**

Numerical particle-tracking experiments were conducted to investigate the transport of water masses at the surface from areas around the Miyako Islands in the summer season from 2003 to 2009. Surface velocity data were derived from the FRA-JCOPE2 reanalysis product (Miyazawa et al., 2009), which is an eddy-resolving (1/12°) ocean model combined with three-dimensional variational data assimilation (satellites, ARGO floats, and shipboard observations), and is one of the most reliable models for the region around Japan for the above time period. The method of tracking particles was basically the same as in Itoh et al. (2009), but we did not include the random walk for simplicity. The release points of particles were selected at the surface of the model grid points around the coastal waters of the Miyako Islands. We assumed that the particles did not increase, die, or sink from the surface during the experiments. To focus on transport during the summer season (July–September), particles were released one month before the summer (June 1) and were tracked until September 30.

To examine differences in the output depending on the start time within the same

234 year, we also performed experiments starting on June 1, 11, and 21, and July 1 in
235 2009. The ratio of particles that reached areas downstream of the Tokara Strait
236 (hereafter Area K) (Fig. 7), including the particles' entrainment to the Kuroshio, to
237 total particles released from the Miyako Islands was computed in all experiments. It
238 should be noted that these experiments contained the following two uncertainties.
239 First, the distribution of *Trichodesmium* around the islands, which strongly influences
240 the destinations of particles, was not able to be determined in advance.
241 *Trichodesmium* is known to aggregate and not to occur uniformly in the ocean
242 (Capone et al., 1997). Second, the model cannot reproduce the current very close to
243 the islands. If a water mass very near the islands was delivered to the open ocean by
244 tide and/or river plumes that were not considered in the model, seaward dispersion of
245 particles was likely underestimated.
246

247 ## 3. RESULTS

248 ### 3.1. The Kuroshio path and bloom frequency

249 The average surface current field indicated that the main stream of the Kuroshio
250 flowed along the continental shelf in the ECS, and then passed to the south of the
251 Kyushu and Shikoku Islands (Fig. 1b). In addition, the Kuroshio branch bifurcated

252 northward at 25°N and 30°N at the continental shelf. Hence, all of the stations in the
253 ECS were subject to the influence of the Kuroshio. While the northeastward stream of
254 the Kuroshio was prominent in this region, smaller-scale flows and circulations were
255 observed in the areas around and to the southeast of the Ryukyu Islands. In the west of
256 the main stream of the Kuroshio, because the average chl *a* was over 0.15 mg m^{-3} (Fig.
257 S2), the frequency of chl *a* values >0.15 mg m^{-3} was high (Fig. 1b). In contrast, the
258 bloom frequency in the east of the main stream of the Kuroshio differed from the
259 distribution of the average chl *a*; algal blooms occurred frequently in the Ryukyu
260 Islands. Around the Miyako Islands, water of high bloom frequency was located to the
261 west of the islands, extending to the north.
262
263 ### 3.2. Region-wide environmental conditions, *Trichodesmium* spp., and
264 nitrogen fixation
265 The sea surface temperature (SST) ranged from 25.1–30.5°C at all of the stations
266 (Table S1), and there were no significant differences among the areas (p>0.05,
267 Tukey's honestly significant difference [HSD] test). The MLD varied from 12–60 m
268 at all of the stations, and was relatively deep around the Miyako Islands compared to
269 the other areas (Table S1). The surface N+N concentration varied between <3 and 42

nM, except around the Miyako Islands (Shiozaki et al., 2010, 2011) (Table S1). The highest surface N+N concentration (374 nM) was observed at St. T0904 where upwelling occurred (see below). No significant difference in the surface N+N was observed among the four areas (p>0.05, Tukey's HSD test). The surface phosphate concentration varied between <3 and 36 nM at all of the stations (Fig. 2a). The phosphate concentration at the surface and within the MLD was not significantly different among the four areas (p>0.05, Tukey's HSD test). There was a greater increase in the phosphate concentrations below 40–50 m in the ECS compared to the other areas (Fig. 3a–d). Furthermore, the phosphate concentrations below 40–50 m near the Miyako Islands were higher than those in the Kuroshio and the Philippine Sea, which were depleted down to 100 m, except at St. T1004 located near the continental shelf. The N/P (= N+N/phosphate) ratio at the surface varied from 0.28 to 6.40 except at St. T0904 (N/P = 16.3) (Table S1), and no significant differences were observed among the four areas (p > 0.05, Tukey's HSD test). The surface dissolved iron concentration ranged from 0.19 to 0.89 nM at all of the stations (Fig 2b), with no significant spatial differences among the four areas (p>0.05, Tukey's HSD test). The surface dissolved iron concentration at Sts. T0622 and T0907 was elevated to 0.83 nM and 0.89 nM, respectively, with lower salinity water than in the adjacent waters

288 (salinity data are shown in Fig. 4a and Kodama et al., 2011). The nMDS showed that
289 the environmental variables at all stations were the same at the >80% similarity level
290 and were >90 % similar excepting station T0904 (Fig. 5). The ANOSIM indicated no
291 significant differences among the stations ($p > 0.05$).
292 The abundance of *Trichodesmium* spp. was highest at the surface at almost all of
293 the stations during the *Nagasaki-maru* 242 and KT-07-21 cruises (Fig. S3). The
294 surface *Trichodesmium* spp. abundances were positively correlated with the
295 depth-integrated abundances ($r^2 = 0.51$, $p < 0.05$) (Fig. 6a). Thus, the surface
296 abundance was used to discuss the geographical distribution of *Trichodesmium* spp.
297 The *Trichodesmium* spp. abundance at the surface varied widely, and there was no
298 significant difference among the four areas ($p > 0.05$, Tukey's HSD test).
299 *Trichodesmium* spp. were observed at all of the stations in the Kuroshio and around
300 the Miyako Islands, whereas they were not always observed in the ECS and the
301 Philippine Sea (Fig. 2c). The average surface abundance in the Philippine Sea was the
302 lowest among all of the areas (Table 1). The highest abundance of *Trichodesmium* spp.
303 (>20000 filaments L^{-1}) was observed near the Miyako Islands at St. T0906, where
304 they bloomed (see below). Tuft-shaped colonies were found at Sts. T0706, T0723,
305 CK-10, and T0906. The nitrogen fixation rate was highest in the upper 25% light

306 depth, and decreased with increasing depth at all of the stations (Fig. 3e–h). The
307 surface rates were positively correlated with the depth-integrated rates ($r^2 = 0.79$, $p <$
308 0.05) (Fig. 6b), suggesting that the distribution of nitrogen fixation was indexed by
309 the surface activity. Surface and depth-integrated nitrogen fixation ranged from 0.54
310 to 62 nmol N L^{-1} d^{-1} and from 29.5 to 753 μmol N m^{-2} d^{-1}, respectively (Fig. 2d and
311 Table S1). Surface nitrogen fixation in the Philippine Sea was significantly lower than
312 that in the Kuroshio ($p < 0.05$, *t*-test).

313 The surface abundance of *Trichodesmium* spp. in the entire study area was
314 positively correlated with the nitrogen fixation rate at the surface ($r^2 = 0.80$; $p < 0.05$
315 [$r^2 = 0.52$; $p < 0.05$ if the datum taken at the *Trichodesmium*-bloom station T0906 is
316 excluded]) (Fig. 6c), suggesting that they significantly contributed to nitrogen fixation
317 in the study region. However, active nitrogen fixation occurred in the ECS where
318 *Trichodesmium* abundance was low, and hence, the other diazotrophs could also be
319 important for nitrogen fixation.

320

321 ### 3.3. **Observation around the Miyako Islands during the KT-09-17 cruise**

322 The SST was lower to the northwest of the Miyako Islands than in adjacent
323 waters, and chl *a* was enriched in the same location (Fig. 4b,c). Therefore, the

enhanced productivity was probably due to nutrient supply by upwelling. This upwelling generally occurs in the lee of islands (Hasegawa et al., 2009), suggesting that there was a northward current during the cruise. The surface salinity was lower east of the Miyako Islands than in the surrounding waters (Fig. 4a). The absence of any large river on the east side of Miyako-jima Island and the separation of low salinity water from the island suggest that the low salinity was caused by rainfall.

St. T0904 was located near the upwelling water; its SST of 29.0°C was lowest and its surface N+N concentration of 374 nM was highest among all of the stations. However, the N+N concentration at St. T0904 at the surface was higher than that at the subsurface (an approximate depth of 50 m; Fig. S4), indicating that St. T0904 was not located in the middle of the upwelling. At St. T0904, the surface phosphate concentration was also highest (23 nM) and the N/P ratio (=16.3) was higher than the Redfield ratio. With the exception of the surface at St. T0904, the phosphate concentration was low (<3–9 nM) in the upper 50 m, with no noticeable variation among the stations (Fig. 2a). The dissolved iron concentration varied between 0.19 and 0.89 nM at the surface (Fig. 2b). The highest dissolved iron concentration was observed at St. T0907.

During the same cruise, we encountered a *Trichodesmium* spp.-bloom at St.

342 T0906 (Fig. 2c), which had colored water at the surface. The abundance of
343 *Trichodesmium* spp. at St. T0906 was >20,000 filaments L^{-1}, which was far higher
344 than that at other stations (2–102 filament L^{-1}). The nitrogen fixation rate at the
345 surface (61.9 nmol N L^{-1} d^{-1}) of this station was more than 30-fold that just below the
346 surface, and was the highest among all of the stations (Fig. 3h). The diatom
347 abundance was markedly higher at St. T0904 than that at the other stations.
348 *Cylindrotheca closterium* was the most numerically dominant diatom (59%), followed
349 by *Navicula* spp. (23%) and *Nitzschia* spp. (13%). *C. closterium* was not detected at
350 the other stations, indicating that the high chl *a* induced by the island wake effect
351 mainly consisted of diatoms.
352

353 ### 3.4. **Numerical simulation**

354 As the Kuroshio generally flows along the continental slope north of the Miyako
355 Islands (Fig. 1b), particles around the Miyako Islands were not transported along the
356 typical path of the Kuroshio to the northeast, especially at their initial stages (Fig. 7a).
357 Some particles migrated around the Miyako Islands, or turned south after they passed
358 the Tokara Strait. Nevertheless, the particles delivered to Area K east of the Tokara
359 Strait increased as time elapsed, and the ratio of particles delivered to Area K to the

total released particles ranged from 13–56% (30 ± 16%) by day 120 in 2003–2009 (Fig. 7b). The year-to-year variations in the ratio are mainly due to influences of mesoscale eddies as partly seen in the particle trajectories in Fig. 7a, and likely occurred over relatively short time scales (shorter than the seasonal time scale). This is supported by another series of experiments in which particles were released on June 1, 11, and 21, and July 1 in 2009, which yielded ratios of 6.2–38% (22 ± 13%) by day 120 (Fig. S5).

4. DISCUSSION

4.1. Distribution of phosphate and dissolved iron concentrations

Phosphate concentrations were consistently low within the MLD in all of the studied areas, and the maximum abundance of *Trichodesmium* spp. and total nitrogen fixation activity generally occurred near the surface, suggesting that the phosphate conditions for surface *Trichodesmium* spp. and other diazotrophs were similar among all of the areas. Furthermore, with the exception of St. T1004 located near the continental shelf, the vertical distribution of phosphate in the Kuroshio was analogous to that in the Philippine Sea. Therefore, at least in the oceanic region of the two areas, phosphate availability for *Trichodesmium* spp. and the other diazotrophs was similar

throughout the water column.

The surface distribution of the dissolved iron concentration demonstrated no significant variation among the areas. The dissolved iron concentration (0.19–0.89 nM) was higher than that in the western North Pacific subtropical region (0.15–0.4 nM) (Brown et al., 2005). Obata et al. (1997) demonstrated that the vertical distribution of the dissolved iron concentration in the ECS showed two peaks (at the surface and in the deep water), suggesting that aerial dust significantly contributes to the high dissolved iron concentration at the surface in all of our study areas. In accordance with our results, previous modeling studies estimated the amount of dust deposition to be similar in all four areas (Jickells et al., 2005; Mahowald et al., 2009). Therefore, iron availability for *Trichodesmium* spp. and the other diazotrophs was also likely similar across all of the study areas. Iron can be supplied from deep water to the surface by mixing processes (Johnson et al., 1999). However, if this were the case, the nitrate concentration would be expected to increase simultaneously at the surface (Johnson et al., 1999), and we observed no noticeable elevation in N+N in any of the areas, except at St. T0904. High concentrations of dissolved iron (>0.8 nM) corresponded with low salinity at Sts. T0622 and T0907, suggesting that wet deposition was an important process for iron supply. Dry deposition could also be

important since the iron-enriched water at Sts. T0601 and T0715 did not correspond with low salinity.

Satellite data analysis indicated that there was a “pipeline” of material transport from the Miyako Islands to the Kuroshio, and this was supported by numerical simulations. According to the hypothesis of Marumo and Asaoka (1974), the growth of *Trichodesmium* in the Kuroshio could be maintained by the supply of iron and phosphorus from the islands situated along the Kuroshio, and the Miyako Islands were considered a possible nutrient source to the Kuroshio. Hence, assuming this hypothesis to be valid, the iron and phosphate concentrations near the Miyako Islands (especially in our observed area) would be expected to be higher than those in the other areas. However, we observed no significant difference in the iron and phosphate concentrations among the four areas. This suggested that there was no detectable washout of iron and phosphorus from the Miyako Islands during our observations, or that diazotrophs and other phytoplankton exhausted the nutrient supply close to the islands.

4.2. Factors controlling the distributions of *Trichodesmium* spp. and nitrogen fixation

Although there was no statistically significant difference in *Trichodesmium* spp. abundance among the study areas probably because the data were limited and the variation was large, *Trichodesmium* spp. were always observed in the Kuroshio and were abundant at most stations. Furthermore, at St.CK-10 in the East China Sea which is in the Kuroshio branch current, a high abundance of *Trichodesmium* spp. was observed. On the other hand, *Trichodesmium* spp. abundance in the Philippine Sea tended to be lower than in the other areas. Such *Trichodesmium* distribution was also reported in the previous study (Marumo and Asaoka, 1974). The present study also showed lower surface nitrogen fixation in the Philippine Sea compared to that in the Kuroshio ($p < 0.05$, *t*-test). Previous studies demonstrated that *Trichodesmium* spp. flourished in some regions of the subtropical ocean where the iron levels were high (Moore et al., 2009; Shiozaki et al., 2014b), which can be attributed to the high iron requirement of *Trichodesmium* spp. for their growth compared to other diazotrophs and non-diazotrophs (Kustka et al., 2003; Saito et al., 2011). Therefore, the distribution of *Trichodesmium* spp. in the study area was expected to be associated with the dissolved iron concentration at the surface. Furthermore, the iron-enhanced active nitrogen fixation causes phosphorus depletion, and is consequently limited by phosphorus (Mather et al., 2008). No significant differences in surface iron and

phosphate were observed among the study areas, which cannot explain the distribution of *Trichodesmium* spp. and nitrogen fixation in the study region.

Johnson et al. (1999) reported that the iron supply increased around the continental shelf because re-suspension from the bottom to the euphotic zone becomes significant. However, in the continental shelf of the ECS, the abundance of *Trichodesmium* spp. and nitrogen fixation were low (Marumo and Asaoka, 1974; Zhang et al., 2012). Zhang et al. (2012) suggested that the low nitrogen fixation in the continental shelf was attributable to mixing processes and the influence of the Changjiang River. Turbulence near the sea floor influences the surface water in the shallower bottom region (Matsuno et al., 2006), and Zhang et al. (2012) suggested that the physical disturbance reduces diazotrophy since diazotrophs including *Trichodesmium* favor calm seas. Furthermore, the water in the continental shelf of the ECS is strongly influenced by the Changjiang River. The N/P ratio of the Changjiang River plume is significantly higher than the Redfield ratio, which results in phosphorus limitation, and can contribute to the low nitrogen fixation (Zhang et al., 2012). In the present study, despite the fact that the surface phosphate concentration was low throughout the study areas, the N/P ratio was generally lower than the Redfield ratio, suggesting that biological production was limited by the availability of

nitrogen compared to phosphate (Moore et al., 2008, 2013). Furthermore, the insignificant difference in MLD among the ECS, the Kuroshio, and the Philippine Sea (p>0.05; Tukey HSD test) indicated similar vertical mixing conditions. Therefore, the environmental variables related to nitrogen fixation only slightly differed as demonstrated by the nMDS plot..

In our study, we found a *Trichodesmium* spp. bloom near the Miyako Islands. Recent studies demonstrated that *Trichodesmium* spp. thrived near oceanic islands (Shiozaki et al., 2010, 2014c; Dupouy et al., 2011). Given that some aspect of the environment around the islands increases *Trichodesmium* spp. abundance and that they are transported from the islands to the Kuroshio, this can explain why the *Trichodesmium* distribution was not estimated from environmental variables. Accordingly, the low abundance of *Trichodesmium* spp. in the Philippine Sea was likely due to the low density of islands. Furthermore, higher nitrogen fixation in the Kuroshio than in the Philippine Sea might be explained in the same manner. *Trichodesmium* is a major nitrogen fixer in the Kuroshio (Chen et al., 2008, 2014; Shiozaki et al., 2014a), and our results showed that the bulk water nitrogen fixation was positively correlated with *Trichodesmium* abundance.

467 The numerical simulation demonstrated that released particles from the Miyako
468 Islands were generally transported to the northeast and flowed along the Kuroshio
469 during summer between 2003 and 2009. Thus, if *Trichodesmium* increases and active
470 nitrogen fixation usually occurs around the Miyako Islands, the water would be
471 delivered to the Kuroshio. Furthermore, we performed additional particle tracking
472 experiments whose particle release points were set at major islands in the Ryukyu
473 Islands (Amami Islands, Okinawa Main Island, and the Ishigaki Islands) (Figs. S6 and
474 S7). The results demonstrated that the particles released from the other islands of the
475 Miyako Islands were also delivered to the Kuroshio, with some exceptions. Based on
476 the calculations for 2003–2009, 13–56% (30 ± 16%) of particles released from the
477 islands reached Area K by day 120 (Fig. S7).
478 Studies on nitrogen fixation around islands in the study region are fairly limited
479 (Liu et al., 2013), and the present study is the first report of a *Trichodesmium* bloom
480 around islands in the area. The Miyako Islands are surrounded by reefs, and studies
481 have shown that *Trichodesmium* blooms can be associated with reef environments
482 (Bell et al., 1999; McKinna et al., 2011). However, the factors causing the
483 *Trichodesmium* blooms around islands are not well understood (Shiozaki et al.,
484 2014c). Further studies are required to identify which characteristics of the near island

485 environment are important for the growth and/or accumulation of *Trichodesmium* and
486 other diazotrophs.
487
488 ## 5. CONCLUSIONS
489 We hypothesize that the high abundance of *Trichodesmium* spp. and active
490 nitrogen fixation in the Kuroshio were ascribable not to the unique nutrient
491 environment, but rather to the supply of *Trichodesmium* spp. and other diazotrophs
492 from the surrounding islands. The Ryukyu Islands would not be the only islands with
493 abundant *Trichodesmium* spp., as *Trichodesmium* spp. also flourish in the upstream
494 Kuroshio near Luzon Island (Chen et al., 2008). Therefore, the abundance of
495 *Trichodesmium* spp. would be generally increased around islands situated along the
496 Kuroshio, and the abundant *Trichodesmium* spp. would likely be transported to the
497 mainstream of the Kuroshio. *Trichodesmium* is a major diazotroph in the Kuroshio
498 (Chen et al., 2008, 2014; Shiozaki et al., 2014a), and diazotrophy in the Kuroshio is
499 considered to influence the nutrient stoichiometry in the North Pacific (Shiozaki et al.,
500 2010). Thus, our results indicate that phenomena around the islands located along the
501 Kuroshio are important for determining the partial nitrogen inventory in the North
502 Pacific.
503

Author Contributions

T.S., S.T., S.I., and K.F. designed the experiment and T.S., S.T., T.K., X.L., F.H., and K.F. collected the samples at sea. T.S. determined nitrogen fixation and abundance of *Trichodesmium* spp. during the KT-06-21, KT-07-21, KT-09-17, and *Nagasaki-maru* 242 cruises, and X.L. did during the KT-10-19 cruise. T.S. analyzed datasets of satellite and climatological current field. S.T. analyzed concentration of dissolved iron. S.I. performed numerical experiments. T.K. and F.H. determined nutrient concentration. T.S. prepared the manuscript with contributions from all co-authors.

Acknowledgements

We thank J. Ishizaka, the captains, crew members, and participants on board the T/V *Nagasaki-maru* and R/V *Tansei-maru* cruises for their cooperation at sea. Thanks also to K. Hayashizaki for his support in use of the mass spectrometer at Kitasato University, to A. Takeshige and J. Hirai for their valuable comments on biology in the Kuroshio, and to T. Kitahashi for his suggestion on statistical analyses. Comments from two anonymous reviewers greatly improved the paper. We appreciate NASA ocean color processing group for providing the chl *a* data set and Japan Oceanographic Data Center for ADCP data set. This research was financially

522 supported by MEXT grant on Priority Areas (18067006 & 21014006) and by
523 Innovative Areas (24121001, 24121005, & 24121006) and by Grant-in-Aid for JSPS
524 Fellows (25-7341).
525

References

Bell, P.R.F., Elmetri, I., Uwins, P.: Nitrogen fixation by *Trichodesmium* spp. in the central and northern Great Barrier Reef lagoon: relative importance of the fixed-nitrogen load, Mar. Ecol. Progr. Ser., 186, 119-126, 1999.

Brown, M.T., Landing, W.M., Measures, C.I.: Dissolved and particulate Fe in the western and central North Pacific: Results from the 2002 IOC cruise, Geochem. Geophys. Geosyst., 6(10), Q10001, 2005.

Capone, D.G., Zehr, P.J., Paerl, H.W., Bergman, B., Carpenter, E.J.: *Trichodesmium*, a globally significant marine cyanobacterium, Science, 276, 1221-1229, 1997.

Chen, C.T.A.: Distributions of nutrients in the East China Sea and the South China Sea connection, J. Oceanogr., 64, 737-751, 2008.

Chen, Y.L.L., Chen, H.Y., Tuo, S.H., Ohki, K.: Seasonal dynamics of new production from *Trichodesmium* N_2 fixation and nitrate uptake in the upstream Kuroshio and South China Sea basin, Limnol. Oceanogr., 53(5), 1705-1721, 2008.

Chen, Y.L.L., Chen, H.Y., Lin, Y.H., Yong, T.C., Taniuchi, Y., Tuo, S.H.: The relative contributions of unicellular and filamentous diazotrophs to N_2 fixation in the South China Sea and the upstream Kuroshio, Deep-Sea Res. I, 85, 56-71, 2014.

Dabundo, R., Lehmann, M.F., Treibergs, L., Tobias, C.R., Altabet, M.A.: The

544 contamination of commercial $^{15}N_2$ gas stocks with ^{15}N-labeled nitrate and ammonium
545 and consequences for nitrogen fixation measurements, PLoS one, 9(10), e110335,
546 2014.
547 Dupouy, C., Benielli-Gary, D., Neveux, J., Dandonneau, Y., Westberry, T.K.: An
548 algorithm for detecting *Trichodesmium* surface blooms in the South Western Tropical
549 Pacific, Biogeosciences, 8, 3631-3647, 2011.
550 Großkopf, T., Mohr, W., Baustian, T., Schunck, H., Gill, D., Kuypers, M.M.M., Lavik,
551 G., Schmitz, R.A., Wallace, D.W.R., LaRoche, J.: Doubling of marine
552 dinitrogen-fixation rate based on direct measurements, Nature, 488, 361-364, 2012.
553 Hasegawa, D., Lewis, M.R., Gangopadhyay, A.: How islands cause phytoplankton to
554 bloom in their wake, Geophys. Res. Lett., 36, L20605, 2009.
555 Hashihama, F., Furuya, K., Kitajima, S., Takeda, S., Takemura, T., Kanda, J.:
556 Macro-scale exhaustion of surface phosphate by dinitrogen fixation in the western
557 North Pacific, Geophys. Res. Lett., 36, L03610, 2009.
558 Isobe, A.: Recent advances in ocean-circulation research on the Yellow Sea and East
559 China Sea shelves, J. Oceanogr., 64, 569-584, 2008.
560 Itoh, S., Yasuda, I., Nishikawa, H., Sasaki, H., Sasai, Y.: Transport and environmental
561 temperature variability of eggs and larvae of the Japanese anchovy (*Engraulis*

562 *japonicus*) and Japanese sardine (*Sardinops melanostictus*) in the western North
563 Pacific estimated via numerical particle-tracking experiments, Fish. Oceanogr., 18(2),
564 118-133, 2009.Jickells, T.D., An, Z.S., Andersen, K.K., Baker, A.R., Bergametti, G.,
565 Brooks, N., Cao, J.J., Boyd, P.W., Duce, R.A., Hunter, K.A., Kawahata, H., Kubilay,
566 N., LaRoche, J., Liss, P.S., Mahowald, N., Prospero, J.M., Ridgwell, A.J., Tegen, I.,
567 Torres, R.: Global iron connections between desert dust, ocean biogeochemistry, and
568 climate, Science, 308, 67-71, 2005.
569 Johnson, K.S., Chavez, F.P., Friederich, G.E.: Continental-shelf sediment as a
570 primary source of iron for coastal phytoplankton, Nature, 398, 697-700, 1999.
571 Johnson, K.S., Boyle, E., Bruland, K., Coale, K., Measures, C., Moffett, J.,
572 Aguilar-Islas, A., Barbeau, K., Bergquist, B., Bowie, A., Buck, K., Cai, Y., Chase, Z.,
573 Cullen, J., Doi, T., Elrod, V., Fitzwater, S., Gordon, M., King, A., Laan, P.,
574 Laglera-Baquer, L., Landing, W., Lohan, M., Mendez, J., Milne, A., Obata, H.,
575 Ossiander, L., Plant, J., Sarthou, G., Sedwick, P., Smith, G.J., Sohst, B., Tanner, S.,
576 Van den Berg, S., Wu, J.: The SAFe iron intercomparison cruise: an international
577 collaboration to develop dissolved iron in seawater standards, Eos, 88, 131-132, 2007.
578 Kodama, T., Furuya, K., Hashihama, F., Takeda, S., Kanda, J.: Occurrence of
579 rain-origin nitrate patches at the nutrient-depleted surface in the East China Sea and

580 the Philippine Sea during summer, J. Geophys. Res., 116, C08003, 2011.

581 Kustka, A., Sañudo-Wilhelmy, S., Carpenter, E.J., Capone, D.G., Raven, J.A.: A

582 revised estimate of the iron use efficiency of nitrogen fixation, with special reference

583 to the marine cyanobacterium *Trichodesmium* spp. (Cyanophyta), J. Phycol., 39,

584 12-25, 2003.

585 Lin, I.-I., Hu, C., Li, Y.-H., Ho, T.-Y., Fischer, T.P., Wong, G.T.F., Wu, J., Huang,

586 C.-W., Chu, D.A., Ko, D.S., Chen, J.-P. : Fertilization potential of volcanic dust in the

587 low-nutrient low-chlorophyll western North Pacific subtropical gyre: Satellite

588 evidence and laboratory study, Glob. Biogeochem. Cycles, 25, GB1006,

589 doi:10.1029/2009GB003758, 2011.

590 Liu, X., Furuya, K., Shiozaki, T., Masuda, T., Kodama, T., Sato, M., Kaneko, H.,

591 Nagasawa, M., Yasuda, I.: Variability in nitrogen sources for new production in the

592 vicinity of the shelf edge of the East China Sea in summer, Cont. Shelf Res., 61-62,

593 23-30, 2013.

594 McKinna, L.I.W., Furnas, M.J., Ridd, P.V.: A simple, binary classification algorithm

595 for detection of *Trichodesmium* spp. within the Great Barrier Reef using MODIS

596 imagery, Limnol. Oceanogr.; Methods, 9, 50-66, 2011.

597 Mahaffey, C., Michaels, A.F., Capone, D.G.: The conundrum of marine N_2 fixation,

598 Am. J. Sci., 305, 546-595, 2005.

599 Mahowald, N.M., Engelstaedter, S., Luo, C., Sealy, A., Artaxo, P., Benitez-Nelson, C.,

600 Bonnet, S., Chen, Y., Chuang, P.Y., Cohen, D.D., Dulac, F., Herut, B., Johansen,

601 A.M., Kubilay, N., Losno, R., Maenhaut, W., Paytan, A., Prospero, J.M., Shank, L.M.,

602 Siefert, R.L.: Atmospheric iron deposition: Global distribution, variability, and human

603 perturbations, Annu. Rev. Mar. Sci., 1, 245-278, 2009.

604 Marumo, R., Asaoka, O.: *Trichodesmium* in the East China Sea 1. Distribution of

605 *Trichodesmium thiebautii* GOMONT during 1961-1967, J. Oceanogr. Soc. Japan, 30,

606 298-303, 1974.

607 Mather, R.L., Reynolds, S.E., Wolff, G.A., Williams, R.G., Torres-Valdes, S.,

608 Woodward, E.M.S., Landolfi, A., Pan, X., Sanders, R., Achterberg, E.P.: Phosphorus

609 cycling in the North and South Atlantic Ocean subtropical gyres, Nat. Geosci., 1,

610 439-443, 2008.

611 Matsuno, T., Lee, J.S., Shimizu, M., Kim, S.H., Pang, I.C.: Measurements of the

612 turbulent energy dissipation rate ε and an evaluation of the dispersion process of the

613 Changjiang Diluted Water in the East China Sea, J. Geophys. Res., 111, C11S09,

614 2006.

615 McGowan, J.A.: Oceanic biogeography of the Pacific, in: The microplaleontology of

616 the oceans, Cambridge University Press, Cambridge, 3-74, 1971.

617 Miyazawa, Y., Zhang, R., Guo, X., Tamura, H., Ambe, D., Lee, J.S., Okuno, A.,

618 Yoshinari, H., Setou, T., Komatsu, K.: Water mass variability in the western North

619 Pacific detected in a 15-year eddy resolving ocean reanalysis, J. Oceanogr., 65,

620 737-756, 2009.

621 Mohr, W., Großkopf, T., Wallace, D.W.R., LaRoche, J.: Methodological

622 underestimation of oceanic nitrogen fixation rate, PLoS one, 5(9), e12583, 2010.

623 Montoya, J.P., Voss, M., Kähler, P., Capone, D.G.: A simple, high-precision,

624 high-sensitivity tracer assay for N_2 fixation, Appl. Environ. Microbiol., 62(3),

625 986-993, 1996.

626 Moore, C.M., Mills, M.M., Langlois, R., Milne, A., Achterberg, E.P., LaRoche, J.,

627 Geider, R.J.: Relative influence of nitrogen and phosphorus availability on

628 phytoplankton physiology and productivity in the oligotrophic sub-tropical North

629 Atlantic Ocean, Limnol. Oceanogr., 53(1), 291-305, 2008.

630 Moore, C.M., Mills, M.M., Achterberg, E.P., Geider, R.J., LaRoche, J., Lucas, M.I.,

631 McDonagh, E.L., Pan, X., Poulton, A.J., Rijkenberg, M.J.A., Suggett, D.J., Ussher,

632 S.J., Woodward, E.M.S.: Large-scale distribution of Atlantic nitrogen fixation

633 controlled by iron availability, Nat. Geosci., 2, 867-871, 2009.

634 Moore, C.M., Mills, M.M., Arrigo, K.R., Berman-Frank, I., Bopp, L., Boyd, P.W.,
635 Galbraith, E.D., Geider, R.J., Guieu, C., Jaccard, S.L., Jickells, T.D., LaRoche, J.,
636 Lenton, T.M., Mahowald, N.M., Marañon, E., Marinov, I., Moore, J.K., Nakatsuka, T.,
637 Oschlies, A., Saito, M.A., Thingstad, T.F., Tsuda, A., Ulloa, O.: Processes and
638 patterns of oceanic nutrient limitation, Nat. Geosci., 6, 701-710, 2013.
639 Obata, H., Karatani, H., Nakayama, E.: Automated determination of iron in seawater
640 by chelating resin concentration and chemiluminescence detection, Anal. Chem., 65,
641 1524-1528, 1993.
642 Obata, H., Karatani, H., Matsui, M., Nakayama, E.: Fundamental studies for chemical
643 speciation of iron in seawater with an improved analytical method, Mar. Chem., 56,
644 97-106, 1997.
645 Saito, M.A., Bertrand, E.M., Dutkiewicz, S., Bulygin, V.V., Moran, D.M., Monteiro,
646 F.M., Follows, M.J., Valois, F.W., Waterbury, J.B.: Iron conservation by reduction of
647 metalloenzyme inventories in the marine diazotroph *Crocosphaera watsonii*, Proc.
648 Natl. Acad. Sci. USA, 108, 2184-2189, 2011.
649 Shiozaki, T., Furuya, K., Kodama, T., Takeda, S.: Contribution of N_2 fixation to new
650 production in the western North Pacific Ocean along 155ºE, Mar. Ecol. Progr. Ser.,
651 377, 19-32, 2009.

652 Shiozaki, T., Furuya, K., Kodama, T., Kitajima, S., Takeda, S., Takemura, T., Kanda,
653 J.: New estimation of N_2 fixation in the western and central Pacific Ocean and its
654 marginal seas,. Glob. Biogeochem. Cycles, 24, GB1015, 2010.
655 Shiozaki, T., Furuya, K., Kurotori, H., Kodama, T., Takeda, S., Endoh, T., Yoshikawa,
656 Y., Ishizaka, J., Matsuno, T.: Imbalance between vertical nitrate flux and nitrate
657 assimilation on a continental shelf: Implications of nitrification, J. Geophys. Res., 116,
658 C10031, 2011.
659 Shiozaki, T., Chen, Y.L.L., Lin, Y.H., Taniuchi, Y., Sheu, D.S., Furuya, K., Chen,
660 H.Y.: Seasonal variations of unicellular diazotroph groups A and B, and
661 *Trichodesmium* in the northern South China Sea and neighboring upstream Kuroshio
662 Current, Cont. Shelf Res., 80, 20-31, 2014a.
663 Shiozaki, T., Ijichi, M., Kodama, T., Takeda, S., Furuya, K.: Heterotrophic bacteria as
664 major nitrogen fixers in the euphotic zone of the Indian Ocean, Glob. Biogeochem.
665 Cycles, 28, 1096-1110, 2014b.
666 Shiozaki, T., Kodama, T., Furuya, K.: Large-scale impact of the island mass effect
667 through nitrogen fixation in the western South Pacific Ocean, Geophys. Res. Lett., 41,
668 2907-2913, 2014c.
669 Wilson, C., Qiu, X.: Global distribution of summer chlorophyll blooms in the

oligotrophic gyres, Progr. Oceanogr., 78, 107-134, 2008.

Zhang, R., Chen, M., Cao, J., Ma, Q., Yang, J., Qiu, Y.: Nitrogen fixation in the East China Sea and southern Yellow Sea during summer 2006, Mar. Ecol. Progr. Ser., 447, 77-86, 2012.

675 Table 1 Summary of *Trichodesmium* at the surface, and depth-integrated nitrogen

676 fixation and its related parameters in the four representative study areas.

Area	*Trichodesmium*[*] [filaments l^{-1}]	N_2 fixation [μmolN L^{-1} d^{-1}]	Temperature[*] [ºC]	MLD [m]	$NO_3^-+NO_2^{-*,†}$ [nM]	$PO_4^{3-*,†}$ [nM]	DFe[*] [nM]
East China Sea	21±58	170±140	28.5±1.2	24±12	19±11	15±9	0.76±0.18
Kuroshio	43±33	199±142	29.4±0.81	27±8	9±8	15±7	0.45±0.13
Philippine Sea	8±8	58.3±25.1	29.4±0.1	23±3	8±3	14±19	0.51±0.25
Miyako Islands	3019±8478	201±274	29.3±0.3	40±12	61±128	8±7	0.38±0.24

677 [*] values in surface water

678 [†]When the concentration was below the detection limit (3 nM), we assumed a concentration of 3 nM to

679 calculate the mean.

680

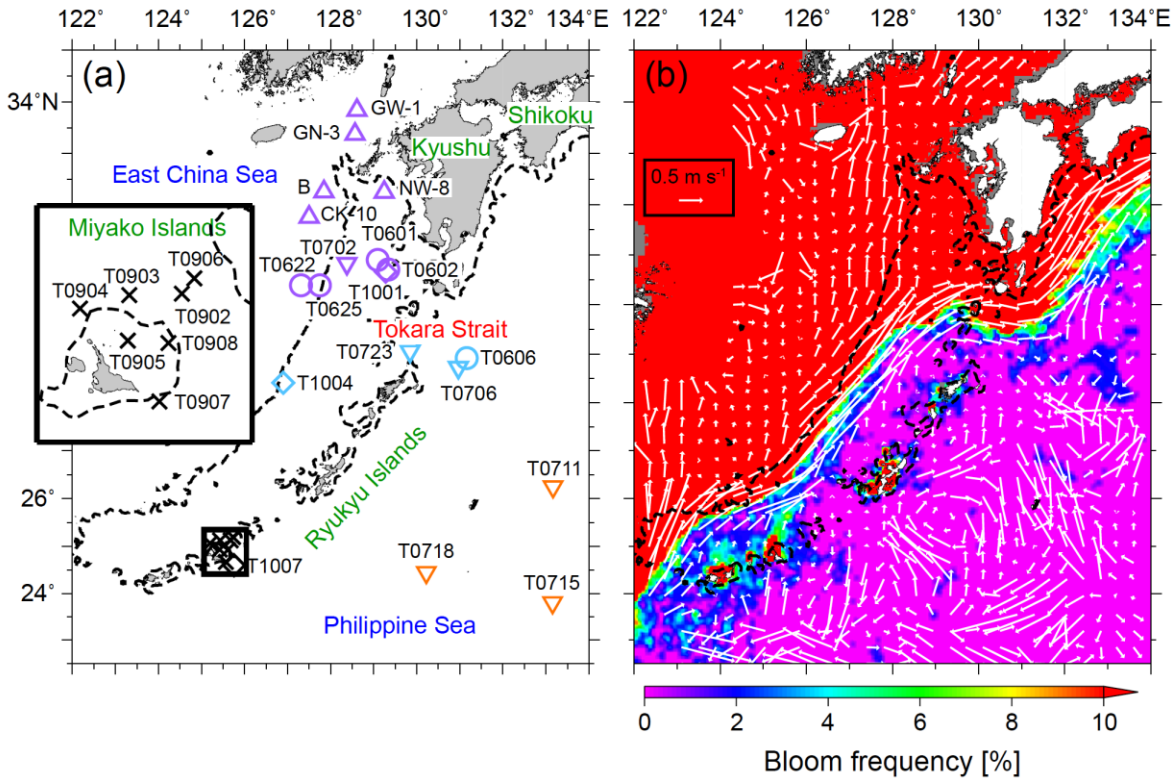

681

682

683 Figure 1. (a) Sampling stations during the KT-06-21 (circles), KT-07-22 (inverted
684 triangles), KT-09-17 (crosses), KT-10-19 (diamonds), and 242 (triangles) cruises.
685 Symbols of stations located in the East China Sea, the Kuroshio, the Philippine Sea,
686 and near the Miyako Islands are indicated in purple, light blue, orange, and black,
687 respectively. (b) Climatological surface current fields during summer (1953–2008)
688 from geoelectrokinetograph measurements and ship-mounted ADCP data. The
689 background contour represents the percentage of chlorophyll *a* of >0.15 mg m^{-3}
690 during summer between 2003 and 2009. Dashed lines indicate 200 m isobaths.

691

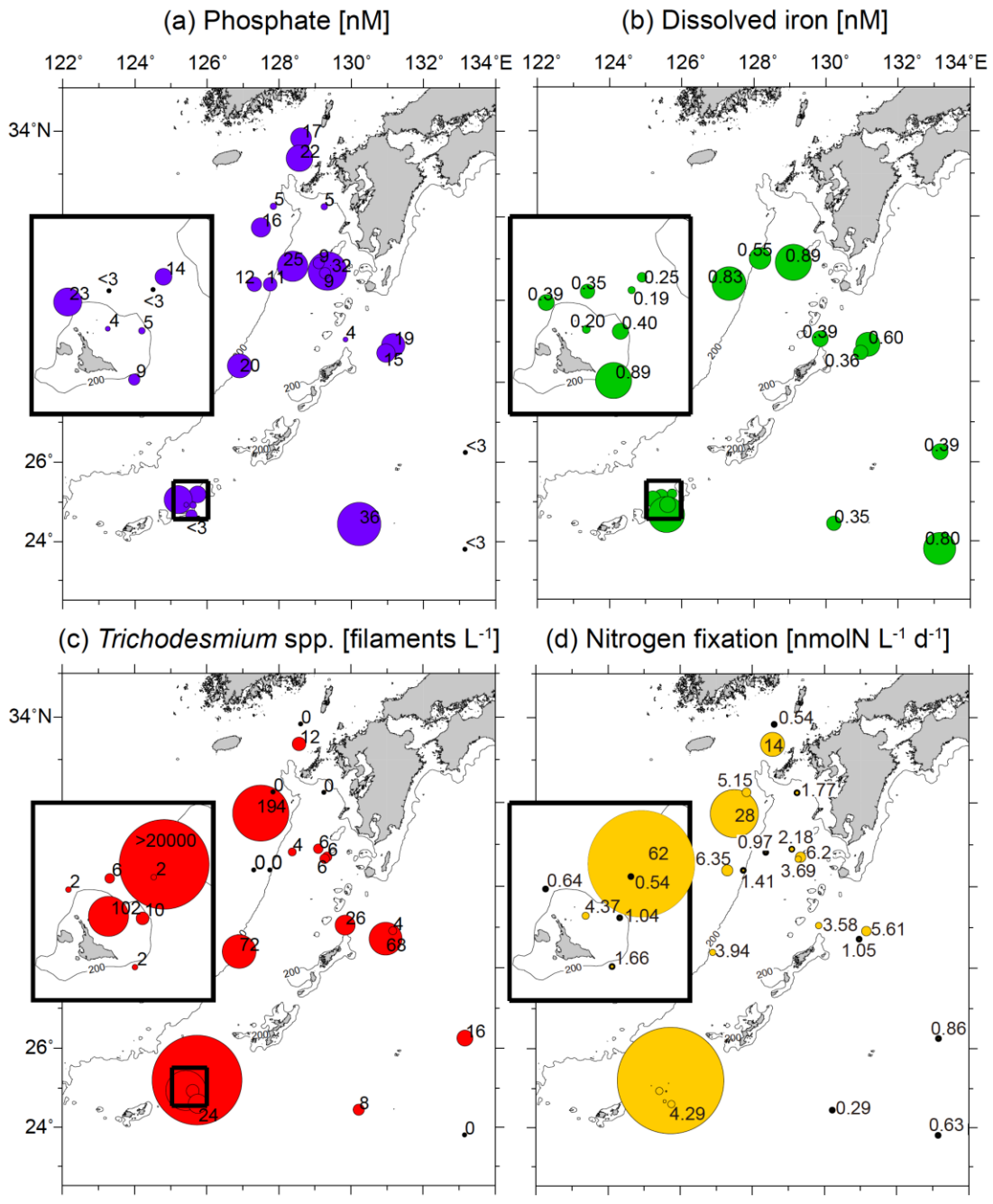

692

693

694 Figure 2. Distribution of (a) phosphate, (b) dissolved iron, (c) *Trichodesmium* spp.,

695 and (d) nitrogen fixation at the surface. The parameters in the small boxes indicate

696 results from the KT-09-17 cruise. The areas of the circles are proportional to the

697 concentration, abundance, or activity.

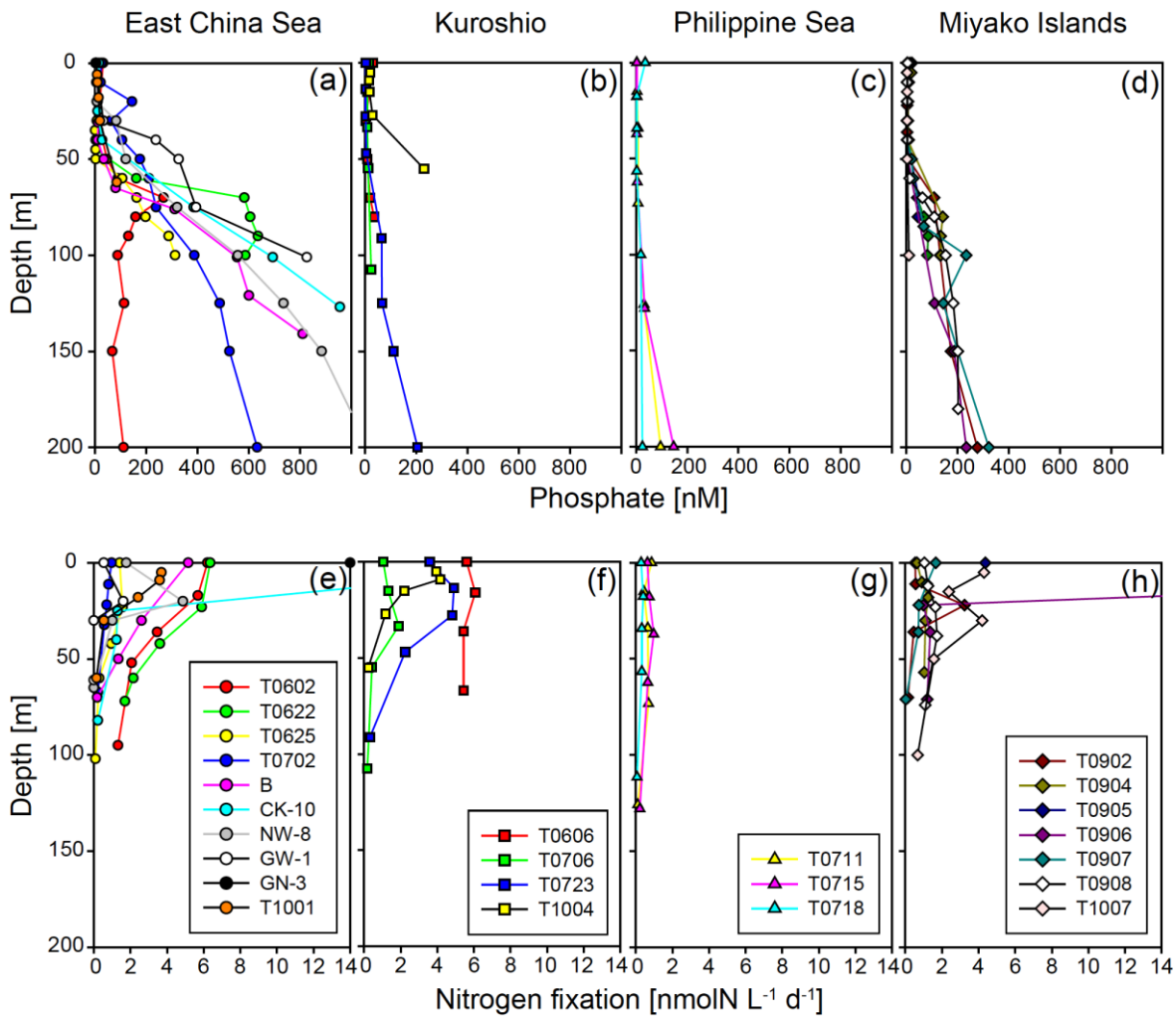

698

699

700 Figure 3. Vertical profiles of phosphate and nitrogen fixation in the East China Sea (a

701 and e), the Kuroshio (b and f), the Philippine Sea (c and g), and the Miyako Islands (d

702 and h).

703

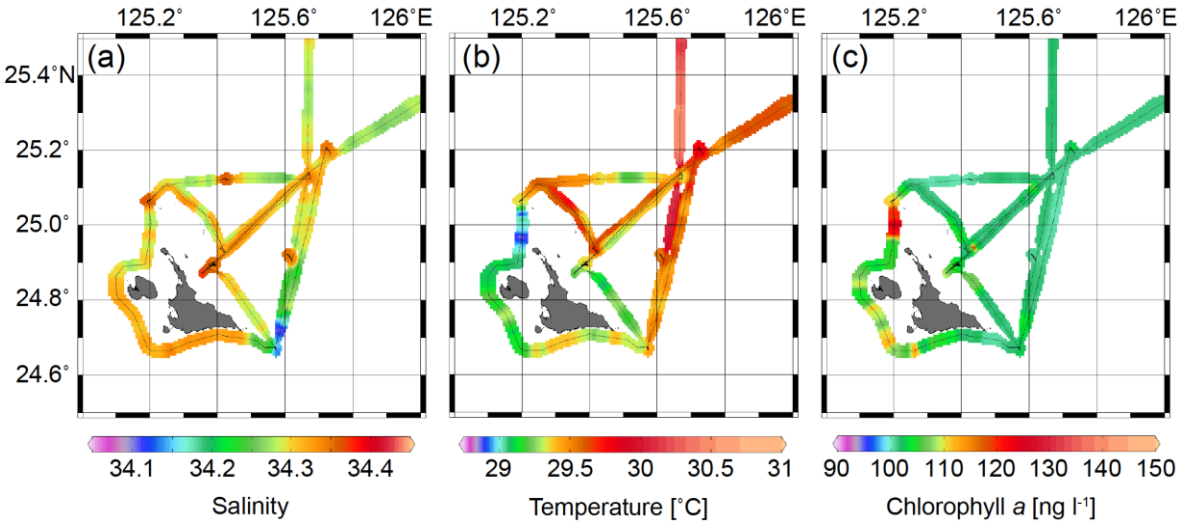

704

705

706 Figure 4. Surface (a) salinity, (b) temperature, and (c) chlorophyll *a* during the

707 KT-09-17 cruise.

708

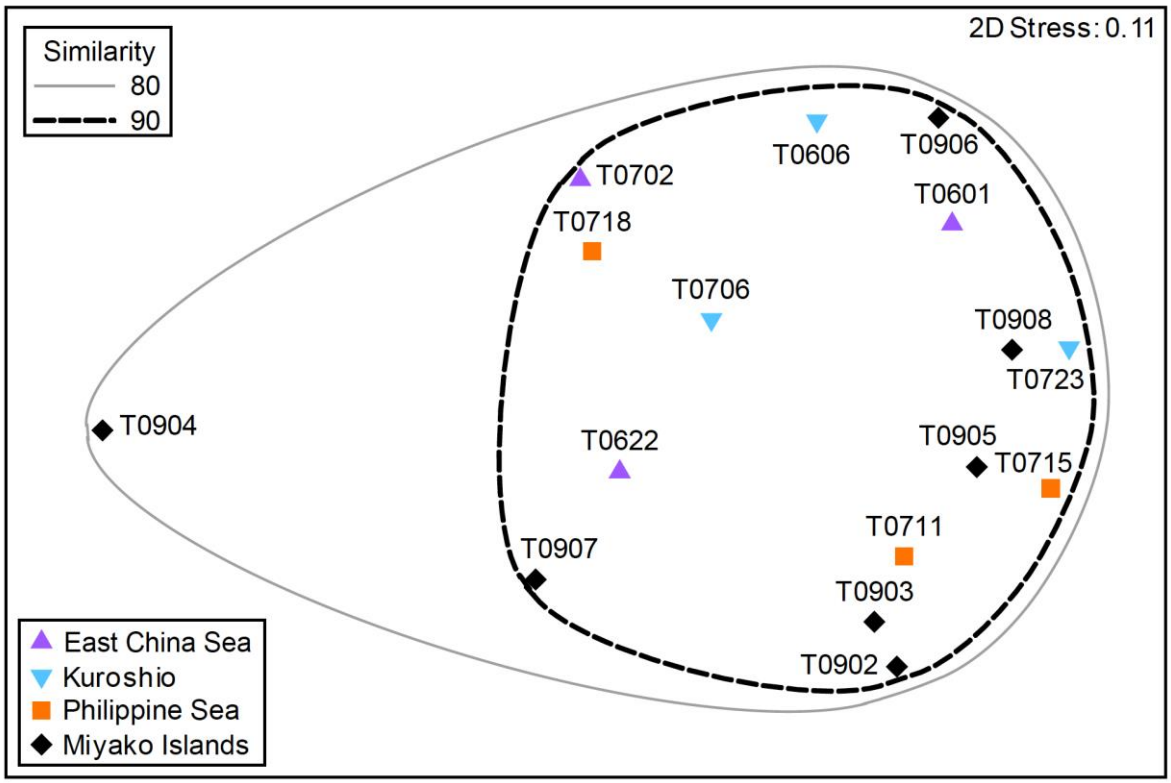

709

710

711 Figure 5. nMDS ordination of sampling stations with environmental variables

712

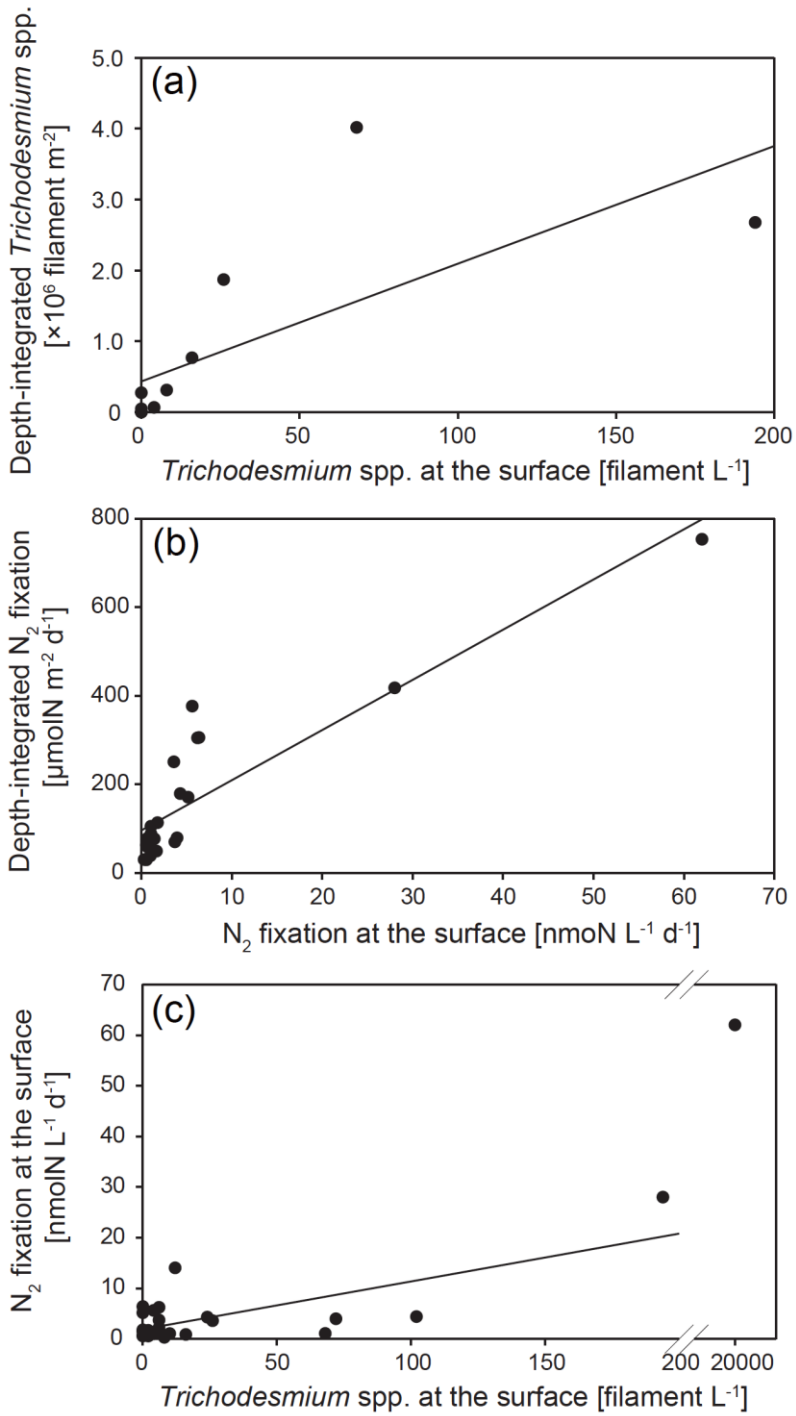

713

714

715 Figure 6. Relationships (a) between surface and depth-integrated *Trichodesmium* spp.

716 abundance, (b) between surface and depth-integrated nitrogen fixation rates, and (c)

717 between *Trichodesmium* spp. abundance and nitrogen fixation rate at the surface.

718

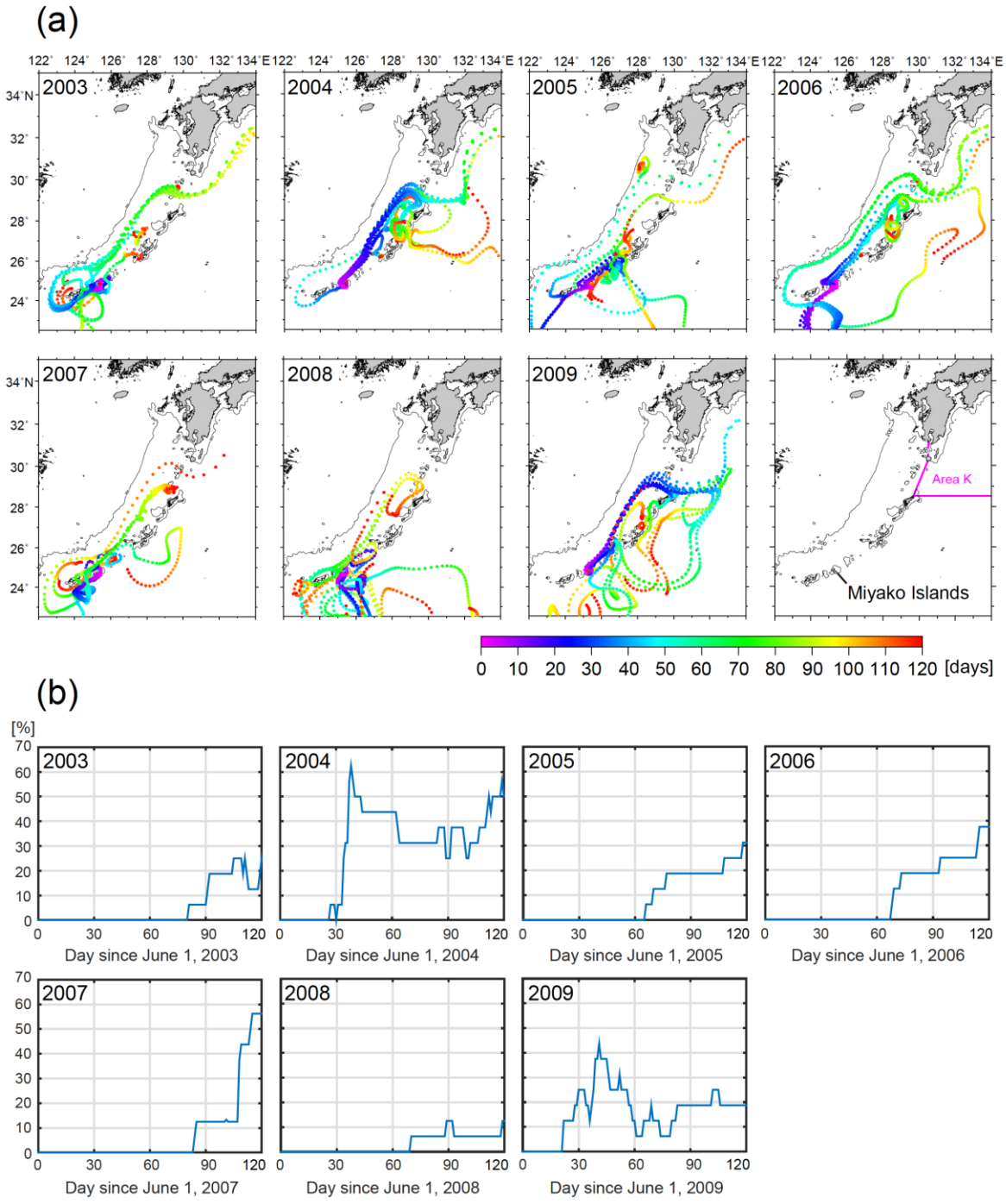

Figure 7. (a) Trajectories of particles released from points around the Miyako Islands on June 1, 2003–2009. (b) The ratio of particles delivered to Area K to the total released particles.